Editors' Suggestion

Dimensionality-Driven Photoproduction of Massive Dirac Pairs near Threshold in Gapped Graphene Monolayers

A. Golub, R. Egger, C. Müller, and S. Villalba-Chávez
Institut für Theoretische Physik, Heinrich Heine Universität Düsseldorf, Universitätsstraße 1, 40225 Düsseldorf, Germany

(Received 19 December 2019; accepted 21 February 2020; published 18 March 2020)

Generation of quasiparticle-hole pairs in gapped graphene monolayers in the combined field of two counterpropagating light waves is studied. The process represents an analog of electron-positron pair production from the vacuum of quantum electrodynamics (QED) by the Breit-Wheeler effect. We show, however, that the two-dimensional structure of graphene causes some striking differences between both scenarios. In particular, contrary to the QED case, it allows for nonzero pair production rates at the energy threshold when the Breit-Wheeler reaction proceeds nonlinearly with absorption of three photons.

DOI: 10.1103/PhysRevLett.124.110403

Introduction.—When atoms or molecules interact with strong laser fields, nonlinear processes relying on the absorption of multiple photons can occur due to the very high photon densities in the field. A variety of strong-field phenomena were discovered, ranging from multiphoton ionization to high-harmonic generation [1], which have paved the way towards new research areas [2].

In recent years there has been a growing interest in interactions of intense laser fields with condensed matter systems [3]. While some of the basic strong-field concepts established in atomic physics can be applied to solids as well [4,5], their more complex electronic structure renders laser-solid interactions generally more involved. In particular, condensed-matter systems can be distinguished by the geometric arrangement of atoms, the symmetry and topology of the band structure, and the behavior of electrons therein. The question thus arises which signatures may emerge in intense laser-solid interactions from the characteristic properties of the system. For example, distinct topological effects from edge states in linear chains have recently been predicted for the strong-field process of high-harmonic generation in solids [6].

A solid-state system of special relevance for strong-field studies is graphene [7] because it can withstand high laser intensities. It is distinguished by its two-dimensional geometry, forming a monolayer of carbon atoms, and its peculiar electronic properties. At zero chemical potential, the electrons in a vicinity of the Fermi surface exhibit a dispersion relation like Dirac fermions, with the speed of light c replaced by the Fermi velocity $v_F \approx c/300$. Recent experiments have demonstrated coherent control of electron dynamics in graphene by driving Landau-Zener transitions with phase-stabilized short laser pulses [8], including the passage from the weak-field to the strong-field regime [9]. Field-driven acceleration of Dirac fermions, which also exist in topological insulators [10], has been observed by combined irradiation of bismuth-telluride surfaces with intense terahertz and short ultraviolet pulses [11].

Graphene moreover serves as a test ground for strong-field processes from the realm of quantum electrodynamics (QED). Fundamental phenomena, such as Klein tunneling [12], Casimir force [13], or Coulomb supercriticality [14], find their low-energy counterpart in graphene. Theoreticians have also discovered graphene as a means to study the Schwinger effect, i.e., the spontaneous production of electron-positron pairs in a constant electric field E_0 [15–22]. The similarity with QED is particularly close in band gap graphene where the quasiparticles acquire a nonzero mass [23]. The Schwinger rate has the characteristic form $\mathcal{R}_S \sim E_0^\nu \exp(-\pi E_c/E_0)$ with the critical field strength E_c associated with the particle mass. The different geometry of the underlying vacuum state only exerts a minor impact here by changing the power of the pre-exponential factor from $\nu = 2$ in QED to $\nu = 3/2$ in graphene [15,21].

In this Letter, we study another strong-field process in graphene which has its counterpart in QED. When a graphene sheet is exposed to the electromagnetic field of two counterpropagating light waves, quasiparticle-hole pairs can be generated by photon absorption (see Fig. 1). This process represents the analog of (non)linear Breit-Wheeler [(N)LBW] pair production from the QED vacuum [24–27]. It may be written symbolically as

$$nk + k' \to p_- + p_+, \tag{1}$$

where n denotes the number of photons with wave vector k from a strong laser field and k' is the wave vector of a weak counterpropagating wave, whereas $p_\pm$ stand for the momenta of created electron and hole, respectively. The NLBW process of QED was observed in an intermediate coupling regime ($n \sim 5$) in collisions of a highly relativistic

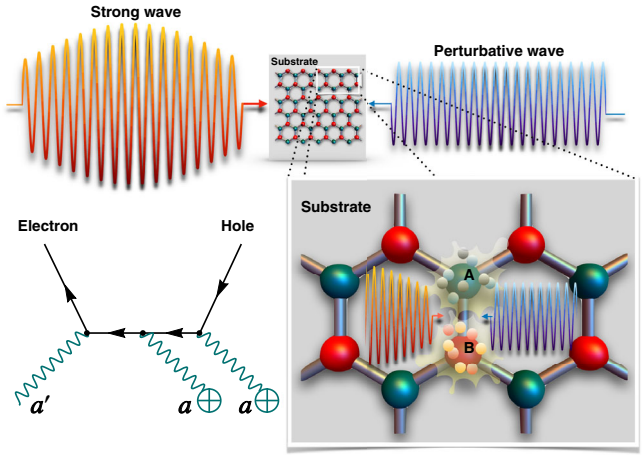

FIG. 1. Scheme of Breit-Wheeler-type production of massive Dirac pairs in a gapped graphene monolayer. The enlarged section illustrates graphene's honeycomb lattice composed of two sublattices A and B. The reciprocal lattice in momentum space is hexagonal, as well, with inequivalent $\boldsymbol{K}$ and $\boldsymbol{K}'$ points in the corners [7]. A representative Feynman diagram is shown which contributes to the three-photon reaction; the wavy lines indicate photons absorbed from fields a' and a, respectively, with the latter being treated as a classical source as marked by the crosses.

electron beam with an intense optical laser pulse [27]. The original (i.e., linear) Breit-Wheeler process with $n = 1$ [24], however, has not been measured yet. Corresponding theoretical proposals to facilitate its detection have been made in recent years, which rely on various kinds of gamma-ray sources in the MeV-GeV energy range [28–31]. Here we provide a theoretical description of the (N)LBW process in gapped graphene monolayers and show that, in principle, they can offer a low-energy alternative, similarly to the Schwinger effect [15–22]. However, our analysis also reveals pronounced qualitative differences with the QED case, which emerge from the two-dimensional structure of graphene.

Planck's constant and the vacuum permittivity are set to unity, $\hbar = \epsilon_0 = 1$, to simplify notation. The speed of light in vacuum is denoted by c and the electron charge and mass by e and m_e, respectively.

Theoretical considerations.—An effective field theoretical framework—that suitably incorporates the electron-hole symmetry predicted within the nearest-neighbor tight-binding model [32] under the assumptions of zero temperature and chemical potential—is adopted. It relies on a Lagrangian density in which the interplay between massive Dirac quasiparticles and an electromagnetic potential $\mathcal{A}_\mu(x)$ [$\mathcal{A}_0(x) = 0$], with $\mu = 0, 1, 2$, $x = (ct, \boldsymbol{x})$ and $\boldsymbol{x} = (\mathsf{x}, \mathsf{y})$, occurs via a minimal coupling [33,34]:

$$\mathcal{L} = \sum_{\sigma=\pm1} \bar{\Psi}_\sigma \left[i\tilde{\gamma}^0 \partial_t + v_F \tilde{\gamma}^j \left(i\partial_j - \frac{e}{c}\mathcal{A}_j \right) - \Delta \right] \Psi_\sigma. \quad (2)$$

Here, $\bar{\Psi}_\sigma = \Psi_\sigma^\dagger \tilde{\gamma}^0$, $\Psi_\sigma^T = (\psi_{\sigma,\boldsymbol{K}}^T, \psi_{\sigma,\boldsymbol{K}'}^T)$ is a four-component spinor consisting of two two-component irreducible pieces corresponding to the $\boldsymbol{K}$ and $\boldsymbol{K}'$ points of the Fermi surface. The spinors $\psi_{\sigma,\boldsymbol{K}}^T = (\psi_{\sigma,\boldsymbol{K},A}, \psi_{\sigma,\boldsymbol{K},B})$, $\psi_{\sigma,\boldsymbol{K}'}^T = (i\psi_{\sigma,\boldsymbol{K}',B}, -i\psi_{\sigma,\boldsymbol{K}',A})$ combine Bloch states associated with the two different sublattices in graphene linked to atoms A and B, whereas the electron spin is included via an additional particle flavor σ. The gamma matrices $\tilde{\gamma}^\mu$ form a reducible 4×4 representation, satisfying $\{\tilde{\gamma}^\mu, \tilde{\gamma}^\nu\} = 2g^{\mu\nu}\mathbb{1}_{4\times4}$ with the metric tensor $g^{\mu\nu} = \mathrm{diag}(1, -1, -1)$. Explicitly, we take $\tilde{\gamma}^\mu = \tau \otimes (\gamma^1, \gamma^2, \gamma^3)$ with $\tau = \sigma_3$, $\gamma^\mu = (\sigma_3, i\sigma_2, -i\sigma_1)$, and the Pauli matrices σ_ℓ, $\ell = 1, 2, 3$. The matrices τ and γ^μ act in the spaces of $\boldsymbol{K}$, $\boldsymbol{K}'$ points and A, B sublattices, respectively. Moreover, in Eq. (2) a sum over the repeated index $j \in \{1, 2\}$ is implied and we introduce a half band gap $\Delta = m_g v_F^2$, which leads to a relativisticlike dispersion relation for quasiparticles $\varepsilon_{\boldsymbol{p}} = \sqrt{v_F^2 \boldsymbol{p}^2 + \Delta^2}$ relative to the Fermi level [22,23]. Likewise, the momentum $\boldsymbol{p} = (p_x, p_y)$ has to be understood relative to the $\boldsymbol{K}$ and $\boldsymbol{K}'$ points, satisfying the condition $|\boldsymbol{p}| \ll p_{\max} \approx |\boldsymbol{K}|, |\boldsymbol{K}'| \approx 3\ \mathrm{eV}/v_F$.

While the fermion states are spatially constrained to the graphene plane, the electromagnetic field extends over all three space dimensions. $\mathcal{A}_\mu(x)$ in Eq. (2) denotes the value of the associated vector potential on the x-y plane. In the following, $\mathcal{A}_\mu(x) = a_\mu(x) + a'_\mu(x)$ is composed of two counterpropagating electromagnetic plane waves $\boldsymbol{a}(x) = \mathfrak{a}_0 \boldsymbol{\epsilon} \cos(kx)$ and $\boldsymbol{a}'(x) = \mathfrak{a}'_0 \boldsymbol{\epsilon}' \cos(k'x)$, with wave vectors $k^\mu = (\omega/c, \boldsymbol{k})$, $k'^\mu = (\omega'/c, \boldsymbol{k}')$ and polarization vectors $\boldsymbol{\epsilon}$, $\boldsymbol{\epsilon}'$ satisfying the transversality relations $\boldsymbol{k} \cdot \boldsymbol{\epsilon} = \boldsymbol{k}' \cdot \boldsymbol{\epsilon}' = 0$. The amplitudes are supposed to fulfill the condition $\eta_g \gg \eta'_g$, in terms of the graphene-modified intensity parameters $\eta_g^{(\prime)} = |e|\mathfrak{a}_0^{(\prime)}/(m_g v_F c)$. We will restrict ourselves to the situation in which both the propagation and polarization directions of the electromagnetic waves lie in the plane of graphene (see Fig. 1) [35]. The chosen field configuration maximizes the photon energy and field amplitudes which are available for pair production in the graphene layer (nonparallel polarization geometries are briefly considered in the Supplemental Material [36]).

Being interested in the intensity regime where η_g, $\eta'_g \ll 1$, we calculate the probability for (N)LBW pair production in graphene (1) by applying perturbation theory in both fields. Observe that, as $\eta_g \gg \eta'_g$, the effect of the strong plane wave can be investigated via coherent states, which is equivalent to considering the corresponding field as a classical background [37]. Hence, the corresponding scattering operator reads

$$\mathcal{S} = \hat{T} \exp\left[ie \frac{v_F}{c} \sum_{\sigma=\pm1} \int dt d^2x (\bar{\psi}_{\sigma,\boldsymbol{K}} \boldsymbol{\gamma} \cdot (\boldsymbol{a} + \boldsymbol{a}') \psi_{\sigma,\boldsymbol{K}} + \bar{\psi}_{\sigma,\boldsymbol{K}'} \boldsymbol{\gamma} \cdot (\boldsymbol{a} + \boldsymbol{a}') \psi_{\sigma,\boldsymbol{K}'}) \right], \quad (3)$$

with $\bar{\psi}_{\sigma,\boldsymbol{K}^{(\prime)}} = \psi^{\dagger}_{\sigma,\boldsymbol{K}^{(\prime)}}\gamma^0$. Here, the field $\boldsymbol{a}'(x)$ is quantized [36] and $\hat{T}$ refers, as usual, to the time-ordering operator. The quantization of the Dirac-like fields $\psi_{\sigma,\boldsymbol{K}}$ and $\psi_{\sigma,\boldsymbol{K}'}$ requires to introduce equal-time anticommutation relations, which preserve the corresponding spin and valley quantum numbers [36]. Accordingly, we can restrict ourselves to S-matrix elements generated by the first term in Eq. (3) and, at the end, multiply the outcome by the spin-valley degeneracy $N_f = 4$.

We remark that the treatment used here differs from the traditional path of analyzing the NLBW process in QED, where the Furry picture, based on exact solutions of the Dirac equation in the presence of a single plane-wave laser field (Volkov states), is applied [25,26]. The corresponding Dirac-like equation in graphene, however, is not solved by Volkov states [38] due to the asymmetry introduced by the Fermi velocity v_F. Besides, we note that pair creation by a *single* photon is kinematically forbidden in gapped graphene (like in QED), whereas in pristine graphene with $\Delta = 0$ it would represent the leading-order production process [39].

Next, we proceed to determine the S-matrix element describing the creation of a quasiparticle with energy momentum $(\varepsilon_{\boldsymbol{p}_-}, \boldsymbol{p}_-)$ and its antiparticle with $(\varepsilon_{\boldsymbol{p}_+}, \boldsymbol{p}_+)$ relative to the $\boldsymbol{K}$ point by the collision of two photons k^μ and k'^μ. In graphene this amplitude reads

$$\begin{aligned}\langle \boldsymbol{p}_+\boldsymbol{p}_-|\mathcal{S}_1|\boldsymbol{k}',\boldsymbol{\epsilon}'\rangle = &-(2\pi)^3 N_+ N_- \frac{e^2\mathfrak{a}_0\mathfrak{a}_0' v_F^2}{4c^2}\mathcal{M}_1 \\ &\times \delta(\varepsilon_{\boldsymbol{p}_+} + \varepsilon_{\boldsymbol{p}_-} - \omega - \omega') \\ &\times \delta^{(2)}(\boldsymbol{p}_+ + \boldsymbol{p}_- - \boldsymbol{k} - \boldsymbol{k}'). \end{aligned} \tag{4}$$

Here, the δ functions encode energy-momentum conservation and $N_\pm = [\Delta/(\varepsilon_{\boldsymbol{p}_\pm} A)]^{1/2}$ are the normalization constants of the quantized Dirac-like field with A referring to the normalization area. Besides, the subscript 1 in the scattering operator and the spinor-matrix product $\mathcal{M}_1$ refers to the number of photons absorbed from the classical source. The latter is given by

$$\begin{aligned}\mathcal{M}_1 = \bar{u}_{\boldsymbol{K}}(\boldsymbol{p}_-)[&\not{\epsilon}' S_{\boldsymbol{K}}(\omega - \varepsilon_{\boldsymbol{p}_+}, \boldsymbol{k} - \boldsymbol{p}_+)\not{\epsilon} \\ &+ \not{\epsilon} S_{\boldsymbol{K}}(\omega' - \varepsilon_{\boldsymbol{p}_+}, \boldsymbol{k}' - \boldsymbol{p}_+)\not{\epsilon}']v_{\boldsymbol{K}}(\boldsymbol{p}_+). \end{aligned} \tag{5}$$

We point out that, in this equation the usual slash notation for products with γ matrices has been employed. While $u_{\boldsymbol{K}}(\boldsymbol{p}_-)$ and $v_{\boldsymbol{K}}(\boldsymbol{p}_+)$ are two-dimensional spinors fulfilling the relations $u_{\boldsymbol{K}}(\boldsymbol{p})\bar{u}_{\boldsymbol{K}}(\boldsymbol{p}) = (\gamma^0\varepsilon_{\boldsymbol{p}} - v_F\boldsymbol{\gamma}\cdot\boldsymbol{p} + \Delta)/(2\Delta)$, $v_{\boldsymbol{K}}(\boldsymbol{p})\bar{v}_{\boldsymbol{K}}(\boldsymbol{p}) = (\gamma^0\varepsilon_{\boldsymbol{p}} - v_F\boldsymbol{\gamma}\cdot\boldsymbol{p} - \Delta)/(2\Delta)$, $S_{\boldsymbol{K}}$ refers to the free propagator linked to the Dirac-like field:

$$S_{\boldsymbol{K}}(\varepsilon,\boldsymbol{p}) = \frac{i}{\gamma^0\varepsilon - v_F\boldsymbol{\gamma}\cdot\boldsymbol{p} - \Delta + i0^+}. \tag{6}$$

The rate of pair production per unit area is obtained by taking the square of the S-matrix element, dividing through the interaction time T_0 and normalization area A, and integrating over the final density of states

$$\mathcal{R}_1^{(2+1)} = N_f \int \frac{Ad^2p_+}{(2\pi)^2}\int \frac{Ad^2p_-}{(2\pi)^2}\frac{|\langle \boldsymbol{p}_+\boldsymbol{p}_-|\mathcal{S}_1|\boldsymbol{k}',\boldsymbol{\epsilon}'\rangle|^2}{T_0 A}. \tag{7}$$

The field frequencies are assumed to be chosen such that the integrals are restricted to regions where $|\boldsymbol{p}_\pm| \ll p_{\max}$. Equation (7) contains the term $|\mathcal{M}_1|^2$ which can be rewritten as a trace over the 2×2-gamma matrices. We point out that, due to their reduced dimensionality, several relations—which are needed to evaluate the trace—differ from the familiar QED_{3+1} case. For instance, while in $3+1$ dimensions $\mathrm{Tr}[\gamma^\mu\gamma^\nu] = 4g^{\mu\nu}$ and $\mathrm{Tr}[\gamma^\mu\gamma^\nu\gamma^\rho] = 0$, in the case under consideration one has $\mathrm{Tr}[\gamma^\mu\gamma^\nu] = 2g^{\mu\nu}$ and $\mathrm{Tr}[\gamma^\mu\gamma^\nu\gamma^\rho] = -2i\epsilon^{\mu\nu\rho}$, where the totally antisymmetric tensor $\epsilon^{\mu\nu\rho}$ is defined with $\epsilon^{012} = 1$. Having these properties in mind and the fact that $v_F/c \ll 1$, we arrive at [36]

$$\mathcal{R}_1^{(2+1)} \approx \eta_g^2\eta_g'^2 m_g^3 v_F^4 \frac{\mathfrak{r}^2(4+\mathfrak{r}^2)}{4(1+\mathfrak{r}^2)^{5/2}}, \tag{8}$$

where $\mathfrak{r} = |\boldsymbol{p}|/(m_g v_F)$ denotes a dimensionless parameter and $\omega = \omega'$ is assumed, such that $\boldsymbol{p} \equiv \boldsymbol{p}_+ = -\boldsymbol{p}_-$ [40].

A particularly interesting outcome results from the amplitude describing the production of pairs driven by the absorption of two classical photons and a quantized field (see Feynman diagram in Fig. 1):

$$\begin{aligned}\langle \boldsymbol{p}_+\boldsymbol{p}_-|\mathcal{S}_2|\boldsymbol{k}',\boldsymbol{\epsilon}'\rangle = &-i(2\pi)^3 N_+ N_- \frac{e^3\mathfrak{a}_0^2\mathfrak{a}_0' v_F^3}{8c^3}\mathcal{M}_2 \\ &\times \delta(\varepsilon_{\boldsymbol{p}_+} + \varepsilon_{\boldsymbol{p}_-} - 2\omega - \omega') \\ &\times \delta^{(2)}(\boldsymbol{p}_+ + \boldsymbol{p}_- - 2\boldsymbol{k} - \boldsymbol{k}'). \end{aligned} \tag{9}$$

The corresponding production rate $\mathcal{R}_2^{(2+1)}$ is obtained by inserting the expression of $\mathcal{M}_2$ given in Ref. [36] and following the procedure outlined above. Considering the smallness of the parameter $v_F/c \ll 1$ and assuming $\omega' = 2\omega$, we find

$$\mathcal{R}_2^{(2+1)} \approx \eta_g^4\eta_g'^2 m_g^3 v_F^4 \frac{2(4 - 30\mathfrak{r}^2 + 108\mathfrak{r}^4 + 17\mathfrak{r}^6)}{81(1+\mathfrak{r}^2)^{9/2}}. \tag{10}$$

Results and discussion.—Figure 2(a) shows the rates $\mathcal{R}_n^{(2+1)}$ for Breit-Wheeler pair production in graphene near the energy threshold for $n \in \{1,2\}$. When $n = 1$, the rate starts from zero, but for $n = 2$ it attains a nonzero value at the threshold [$\mathcal{R}_2^{(2+1)} \approx 8\eta_g^4\eta_g'^2 m_g^3 v_F^4/81$]. This is in sharp contrast to the rates $\mathcal{R}_n^{(3+1)}$ for the corresponding processes in QED_{3+1} which always vanish at the threshold [41]. Thus, the special geometry of graphene leads to

distinct qualitative changes in the properties of NLBW pair production.

The QED_{3+1} rates scale like $\mathcal{R}_n^{(3+1)} \sim \alpha\eta^{2n}|\boldsymbol{p}|$ for $|\boldsymbol{p}| \to 0$, with $\eta = |e|\mathfrak{a}_0/(m_e c^2) \ll 1$, when the γ beam is unpolarized [see Fig. 2(b)]. This is in accordance with Wigner's well-known theory for the threshold behavior of quantum mechanical scattering processes with two particles in the final state [42]. It arises from an expression of the form $\int d^3p_+ \int d^3p_- |\mathcal{M}|^2 \delta^{(4)}(p_+ + p_- - Q) \propto \int dp_+^0 |\boldsymbol{p}_+| |\mathcal{M}|^2 \delta(p_+^0 + p_-^0 - Q^0) \propto |\boldsymbol{p}_+|$ under the assumption that the squared matrix element $|\mathcal{M}|^2$ behaves like a constant near the threshold.

In the case of graphene, this argument needs to be modified. Because of the reduced dimensionality of the phase space, it reads $\int d^2p_+ \int d^2p_- |\mathcal{M}|^2 \delta^{(3)}(p_+ + p_- - Q) \propto \int dp_+^0 |\mathcal{M}|^2 \delta(p_+^0 + p_-^0 - Q^0) \propto \text{const}$. This explains why the NLBW pair production rate at the threshold can be nonzero in graphene, which occurs when $n = 2$ [see Fig. 2(a)]. A similar phenomenon is known from electron-atom scattering processes occurring in the presence of a strong magnetic field. The field leads to a reduction of the effective dimensionality of the problem and, thus, to a modification of its threshold behavior [43].

Still, the behavior of $\mathcal{R}_n^{(2+1)}$ for $n = 1$ does not follow the same law. Instead one finds $\mathcal{R}_1^{(2+1)} \sim |\boldsymbol{p}|^2$ [see Eq. (8)]. Here, a more complex explanation is required that combines the two-dimensional geometry of graphene with the polarization state of the ω' photon and the fermionic nature of the charge carriers. The pair production rates in graphene rely on incident light waves whose polarization vectors lie in the graphene plane and are parallel to each other. The QED_{3+1} rates resulting from this field configuration are shown in Fig. 2(c). While $\mathcal{R}_n^{(3+1)}$ for $n = 2$ still grows linearly with $|\boldsymbol{p}|$ near the threshold, a cubic dependence $\sim|\boldsymbol{p}|^3$ is found for $n = 1$. The fact that the produced particles are fermions is of crucial importance here. In fact, for scalar particles the rate of the ordinary Breit-Wheeler process is given by $\mathcal{R}_{1,\mathrm{scal}}^{(3+1)} \sim \alpha\eta^2|\boldsymbol{p}|(\boldsymbol{\epsilon}\cdot\boldsymbol{\epsilon}')^2$ [44], which yields a linear dependence on $|\boldsymbol{p}|$ when the photon polarizations are parallel. Instead, the leading-order term for production of Dirac pairs is $\mathcal{R}_1^{(3+1)} \sim \alpha\eta^2|\boldsymbol{p}|(\boldsymbol{\epsilon}\times\boldsymbol{\epsilon}')^2$ which vanishes in case of parallel polarization vectors. The next-to-leading order term grows with $|\boldsymbol{p}|^3$, in accordance with Fig. 2(c). Applying the above argument of reduced phase space to this scaling law gives the threshold behavior $\mathcal{R}_1^{(2+1)} \sim |\boldsymbol{p}|^2$ found in graphene.

We can gain an intuitive understanding of the vanishing and nonvanishing threshold rates in graphene for $n = 1$ and 2, respectively, by considering the total angular momentum in the process. At the threshold, the quasiparticles do not carry orbital angular momentum (since $\boldsymbol{p}_\pm = 0$) and we may assume that the spin is conserved in the electronic transition from valence to conduction band [45], meaning that the total spin of the electron-hole pair is zero. However, its total *pseudospin* is one, as the structure of the matrix elements $\mathcal{M}_1$ and $\mathcal{M}_2$ in combination with the spinors given in Ref. [36] indicates (see also Ref. [39]). According to Ref. [45], the latter is associated with one unit of angular momentum, which must be provided by the absorbed photons. With two photons this is not possible, though, implying that $\mathcal{R}_1^{(2+1)} = 0$ at the threshold. Instead, three photons can generate one unit of angular momentum, so that the corresponding NLBW process is allowed at the threshold and yields $\mathcal{R}_2^{(2+1)} > 0$. The situation resembles the decay of orthopositronium: As a spin-triplet state, it annihilates into three photons because a two-photon decay is forbidden.

An experimental test of our predictions could apply moderately intense beams of terahertz radiation [11,46]. If we assume, for example, a gap parameter $\Delta = 0.1$ eV [23], frequencies $\omega' = 2\omega \gtrsim 0.1$ eV and intensities $I_0 = 10I_0' = 10^5$ W/cm^2 ($\eta_g \approx 0.1$, $\eta_g' \approx 1.6 \times 10^{-2}$), we obtain at the threshold $\mathcal{R}_2^{(2+1)} \approx 10^{10}$ s^{-1} μm^{-2}. We remark that, in order to be consistent with our perturbative treatment, the fields should lie well below the critical field in graphene $E_c = \Delta^2/|e|v_F$ for the considered gap. This value corresponds to the critical intensity $I_c = cE_c^2/2 \approx 6 \times 10^7$ W/cm^2. Detection of the produced pairs could be achieved by

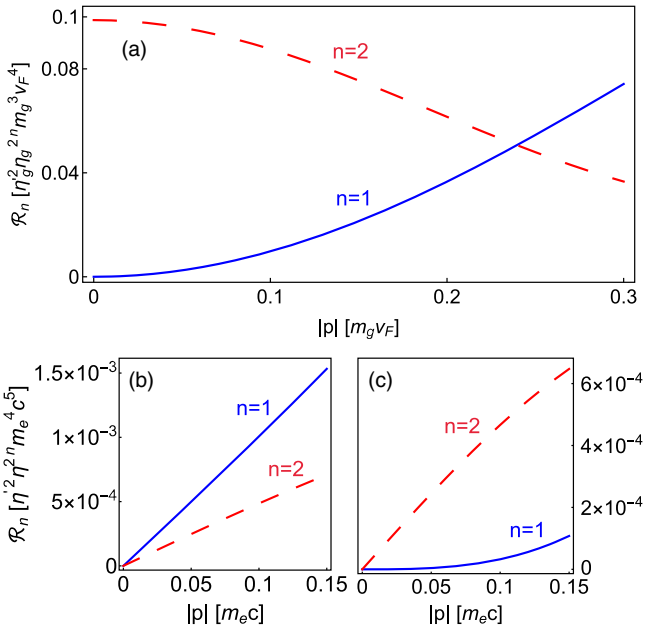

FIG. 2. Near-threshold behavior of the total rates for (N)LBW pair production in the center-of-mass frame, as a function of the absolute value of momentum of one of the created particles: (a) in graphene, (b) in QED_{3+1} with an unpolarized γ photon, (c) in QED_{3+1} with a polarized γ photon, for $n = 1$ (blue solid), $n = 2$ (red dashed).

measuring the induced current when an external voltage is applied [15].

Conclusion and outlook.—Generation of quasiparticle-hole pairs in gapped graphene monolayers by counter-propagating photon beams was studied. The process is analogous to (N)LBW pair production in QED. Focusing on the low-intensity regime at moderate coupling strengths (η_g, $\eta_g' \ll 1$), we revealed striking qualitative differences between both phenomena that are caused by the different dimensionalities of the underlying vacuum state. While the pair production rate at the energy threshold vanishes in QED_{3+1} for any photon number, in graphene it can attain a nonzero value. This result has been shown explicitly for a three-photon reaction and—based on our intuitive angular-momentum consideration—we expect that it holds generally when the total number of absorbed photons is odd. This point will be examined in a forthcoming study.

Future work could, moreover, account for further aspects in the structure of graphene (such as edge states [6]) and its interaction with the external field (such as influences of the substrate on the effective field strength experienced by the charge carriers [8]). However, since the modified threshold behavior results from a basic property of graphene, namely, its two-dimensional geometry, the predicted effects are expected to be robust and to persist in improved treatments. Our results furthermore suggest that the (N)LBW process in topological matter with Dirac-like states might be used to identify domains where quasiparticle-hole generation is restricted to two dimensions (like, e.g., on surfaces).

This work has been funded by the Deutsche Forschungsgemeinschaft (DFG, German Research Foundation) under Grant No. 388720772 (MU 3149/5-1). We thank A. B. Voitkiv for useful discussions.

[1] D. B. Milošević, G. G. Paulus, D. Bauer, and W. Becker, Above-threshold ionization by few-cycle pulses, J. Phys. B **39**, R203 (2006); C. Winterfeldt, C. Spielmann, and G. Gerber, Colloquium: Optimal control of high-harmonic generation, Rev. Mod. Phys. **80**, 117 (2008).

[2] F. Calegari, G. Sansone, S. Stagira, C. Vozzi, and M. Nisoli, Advances in attosecond science, J. Phys. B **49**, 062001 (2016).

[3] S. Ghimire, G. Ndabashimiye, A. D. DiChiara, E. Sistrunk, M. I. Stockman, P. Agostini, L. F. DiMauro, and D. A Reis, Strong-field and attosecond physics in solids, J. Phys. B **47**, 204030 (2014).

[4] G. Vampa, T. J. Hammond, N. Thiré, B. E. Schmidt, F. Légaré, C. R. McDonald, T. Brabec, D. D. Klug, and P. B. Corkum, All-Optical Reconstruction of Crystal Band Structure, Phys. Rev. Lett. **115**, 193603 (2015).

[5] G. Ndabashimiye, S. Ghimire, M. Wu, D. A. Browne, K. J. Schafer, M. B. Gaarde, and D. A. Reis, Solid-state harmonics beyond the atomic limit, Nature (London) **534**, 520 (2016).

[6] D. Bauer and K. K. Hansen, High-Harmonic Generation in Solids With and Without Topological Edge States, Phys. Rev. Lett. **120**, 177401 (2018); H. Drüeke and D. Bauer, Robustness of topologically sensitive harmonic generation in laser-driven linear chains, Phys. Rev. A **99**, 053402 (2019).

[7] A. H. Castro Neto, F. Guinea, N. M. R. Peres, K. S. Novoselov, and A. K. Geim, The electronic properties of graphene, Rev. Mod. Phys. **81**, 109 (2009).

[8] T. Higuchi, C. Heide, K. Ullmann, H. B. Weber, and P. Hommelhoff, Light-field-driven currents in graphene, Nature (London) **550**, 224 (2017); C. Heide, T. Higuchi, H. B. Weber, and P. Hommelhoff, Coherent Electron Trajectory Control in Graphene, Phys. Rev. Lett. **121**, 207401 (2018).

[9] C. Heide, T. Boolakee, T. Higuchi, H. B. Weber, and P. Hommelhoff, Interaction of carrier envelope phase-stable laser pulses with graphene: The transition from the weak-field to the strong-field regime, New J. Phys. **21**, 045003 (2019).

[10] X.-L. Qi and S.-C. Zhang, Topological insulators and superconductors, Rev. Mod. Phys. **83**, 1057 (2011).

[11] J. Reimann *et al.*, Subcycle observation of lightwave-driven Dirac currents in a topological surface band, Nature (London) **562**, 396 (2018).

[12] M. I. Katsnelson, K. S. Novoselov, and A. K. Geim, Chiral tunnelling and the Klein paradox in graphene, Nat. Phys. **2**, 620 (2006).

[13] A. A. Banishev, H. Wen, J. Xu, R. K. Kawakami, G. L. Klimchitskaya, V. M. Mostepanenko, and U. Mohideen, Measuring the Casimir force gradient from graphene on a SiO_2 substrate, Phys. Rev. B **87**, 205433 (2013).

[14] V. M. Pereira, J. Nilsson, and A. H. Castro Neto, Coulomb Impurity Problem in Graphene, Phys. Rev. Lett. **99**, 166802 (2007); I. S. Terekhov, A. I. Milstein, V. N. Kotov, and O. P. Sushkov, Screening of Coulomb Impurities in Graphene, Phys. Rev. Lett. **100**, 076803 (2008).

[15] D. Allor, T. D. Cohen, and D. A. McGady, The Schwinger mechanism and graphene, Phys. Rev. D **78**, 096009 (2008).

[16] M. Lewkowicz and B. Rosenstein, Dynamics of Particle-Hole Pair Creation in Graphene, Phys. Rev. Lett. **102**, 106802 (2009).

[17] B. Dora and R. Moessner, Nonlinear electric transport in graphene: Quantum quench dynamics and the Schwinger mechanism, Phys. Rev. B **81**, 165431 (2010); S. P. Gavrilov, D. M. Gitman, and N. Yokomizo, Dirac fermions in strong electric field and quantum transport in graphene, Phys. Rev. D **86**, 125022 (2012).

[18] G. L. Klimchitskaya and V. M. Mostepanenko, Creation of quasiparticles in graphene by a time-dependent electric field, Phys. Rev. D **87**, 125011 (2013).

[19] H. K. Avetissian, A. K. Avetissian, G. F. Mkrtchian, and Kh. V. Sedrakian, Creation of particle-hole superposition states in graphene at multiphoton resonant excitation by laser radiation, Phys. Rev. B **85**, 115443 (2012).

[20] F. Fillion-Gourdeau and S. MacLean, Time-dependent pair creation and the Schwinger mechanism in graphene, Phys. Rev. B **92**, 035401 (2015).

[21] I. Akal, R. Egger, C. Müller, and S. Villalba-Chávez, Low-dimensional approach to pair production in an oscillating

electric field: Application to bandgap graphene layers, Phys. Rev. D **93**, 116006 (2016).

[22] I. Akal, R. Egger, C. Müller, and S. Villalba-Chávez, Simulating dynamically assisted production of Dirac pairs in gapped graphene monolayers, Phys. Rev. D **99**, 016025 (2019).

[23] Various techniques enable to induce a band gap in graphene, such as epitaxial growth on suitable substrates, elastic strain, or Rashba spin splittings on magnetic substrates; see, e.g., S. Y. Zhou, G.-H. Gweon, A. V. Fedorov, P. N. First, W. A. de Heer, D.-H. Lee, F. Guinea, A. H. Castro Neto, and A. Lanzara, Substrate-induced band gap opening in epitaxial graphene, Nat. Mater. **6**, 770 (2007); A. Varykhalov, J. Sánchez-Barriga, A. M. Shikin, C. Biswas, E. Vescovo, A. Rybkin, D. Marchenko, and O. Rader, Electronic and Magnetic Properties of Quasifreestanding Graphene on Ni, Phys. Rev. Lett. **101**, 157601 (2008); A. K. Geim and I. V. Grigorieva, Van der Waals heterostructures, Nature (London) **499**, 419 (2013); B. Liu and K. Zhou, Recent progress on graphene-analogous 2D nanomaterials: Properties, modeling and applications, Prog. Mater. Sci. **100**, 99 (2019); M. Yankowitz, Q. Ma, P. Jarillo-Herrero, and B. J. LeRoy, van der Waals heterostructures combining graphene and hexagonal boron nitride, Nat. Rev. Phys. **1**, 112 (2019).

[24] G. Breit and J. A. Wheeler, Collision of two light quanta, Phys. Rev. **46**, 1087 (1934).

[25] V. I. Ritus, Quantum effects of the interaction of elementary particles with an intense electromagnetic field, J. Sov. Laser Res. **6**, 497 (1985).

[26] For recent theoretical work on the NLBW process, see the following papers and references cited therein: A. Di Piazza, Nonlinear Breit-Wheeler Pair Production in a Tightly Focused Laser Beam, Phys. Rev. Lett. **117**, 213201 (2016); S. Meuren, K. Z. Hatsagortsyan, C. H. Keitel, and A. Di Piazza, High-Energy Recollision Processes of Laser-Generated Electron-Positron Pairs, Phys. Rev. Lett. **114**, 143201 (2015); M. J. A. Jansen, J. Z. Kaminski, K. Krajewska, and C. Müller, Strong-field Breit-Wheeler pair production in short laser pulses: Relevance of spin effects, Phys. Rev. D **94**, 013010 (2016); Q. Z. Lv, S. Dong, Y. T. Li, Z. M. Sheng, Q. Su, and R. Grobe, Role of the spatial inhomogeneity on the laser-induced vacuum decay, Phys. Rev. A **97**, 022515 (2018); A. I. Titov, H. Takabe, and B. Kämpfer, Nonlinear Breit-Wheeler process in short laser double pulses, Phys. Rev. D **98**, 036022 (2018).

[27] D. L. Burke *et al.*, Positron Production in Multiphoton Light-by-Light Scattering, Phys. Rev. Lett. **79**, 1626 (1997).

[28] O. J. Pike, F. Mackenroth, E. G. Hill, and S. J. Rose, A photon-photon collider in a vacuum hohlraum, Nat. Photonics **8**, 434 (2014); B. King, H. Gies, and A. Di Piazza, Pair production in a plane wave by thermal background photons, Phys. Rev. D **86**, 125007 (2012).

[29] X. Ribeyre, E. d'Humieres, O. Jansen, S. Jequier, V. T. Tikhonchuk, and M. Lobet, Pair creation in collision of γ-ray beams produced with high-intensity lasers, Phys. Rev. E **93**, 013201 (2016).

[30] I. Drebot, D. Micieli, E. Milotti, V. Petrillo, E. Tassi, and L. Serafini, Matter from light-light scattering via Breit-Wheeler events produced by two interacting Compton sources, Phys. Rev. Accel. Beams **20**, 043402 (2017).

[31] J. Q. Yu, H. Y. Lu, T. Takahashi, R. H. Hu, Z. Gong, W. J. Ma, Y. S. Huang, C. E. Chen, and X. Q. Yan, Creation of Electron-Positron Pairs in Photon-Photon Collisions Driven by 10-PW Laser Pulses, Phys. Rev. Lett. **122**, 014802 (2019).

[32] P. R. Wallace, The band theory of graphite, Phys. Rev. **71**, 622 (1947).

[33] S. G. Sharapov, V. P. Gusynin, and H. Beck, Magnetic oscillations in planar systems with Dirac-like spectrum of quasiparticle excitations, Phys. Rev. B **69**, 075104 (2004); V. P. Gusynin and S. G. Sharapov, Transport of Dirac quasiparticles in graphene: Hall and optical conductivities, Phys. Rev. B **73**, 245411 (2006).

[34] In Eq. (2) we neglect the Coulomb interaction between the quasiparticles because it is known to be of minor importance in graphene at low temperatures [see, e.g., L. Fritz, J. Schmalian, M. Müller, and S. Sachdev, Quantum critical transport in clean graphene, Phys. Rev. B **78**, 085416 (2008)].

[35] The magnetic field component is perpendicular to the graphene sheet. In a classical picture, the particle dynamics is thus restricted to the graphene plane since the Lorentz force $\sim \mathbf{p} \times \mathbf{B}$ lies within the plane.

[36] See Supplemental Material at http://link.aps.org/supplemental/10.1103/PhysRevLett.124.110403 for additional details on the theoretical framework and the derivation of our main results.

[37] E. S. Fradkin, D. M. Gitman, and S. M. Shvartsman, *Quantum Electrodynamics with Unstable Vacuum* (Springer-Verlag, Berlin Heidelberg, 1961).

[38] For related problems, see S. Varró, New exact solutions of the Dirac equation of a charged particle interacting with an electromagnetic plane wave in a medium, Laser Phys. Lett. **10**, 095301 (2013); M. Oliva-Leyva and G. G. Naumis, Sound waves induce Volkov-like states, band structure and collimation effect in graphene, J. Phys. Condens. Matter **28**, 025301 (2016).

[39] M. Mecklenburg, J. Woo, and B. C. Regan, Tree-level electron-photon interactions in graphene, Phys. Rev. B **81**, 245401 (2010); M. Lewkowicz, H. C. Kao, and B. Rosenstein, Signature of the Schwinger pair creation rate via radiation generated in graphene by a strong electric current, Phys. Rev. B **84**, 035414 (2011).

[40] Note that the energy-momentum balance for (N)LBW pair production in graphene can be fulfilled by the quasiparticles alone, without participation of the ionic lattice to absorb recoil momentum.

[41] Throughout this Letter, we consider the rates to leading order in the fine-structure constant α. We point out that the Breit-Wheeler rate in QED [24] attains a very small finite threshold value when next-to-leading order corrections in α due to final-state Coulomb interactions are taken into account; see, e.g., R. J. Gould, Born-approximation and radiative corrections to pair production in photon-photon collisions, Astrophys. J. **337**, 950 (1989).

[42] E. P. Wigner, On the behavior of cross sections near threshold, Phys. Rev. **73**, 1002 (1948); L. D. Landau and E. M. Lifshitz, *Quantum Mechanics* (Pergamon, Oxford, 1965).

[43] H. R. Sadeghpour, J. L. Bohn, M. J. Cavagnero, B. D. Esryk, I. I. Fabrikant, J. H. Macek, and A. R. P. Rau, Collisions

near threshold in atomic and molecular physics, J. Phys. B **33**, R93 (2000).

[44] A. I. Akhiezer and V. B. Berestetskii, *Quantum Electrodynamics*, 2nd ed. (Wiley, New York, 1965).

[45] M. Mecklenburg and B. C. Regan, Spin and the Honeycomb Lattice: Lessons from Graphene, Phys. Rev. Lett. **106**, 116803 (2011).

[46] D. J. Cook and R. M. Hochstrasser, Intense terahertz pulses by four-wave rectification in air, Opt. Lett. **25**, 1210 (2000); T. Bartel, P. Gaal, K. Reimann, M. Woerner, and T. Elsaesser, Generation of single-cycle THz transients with high electric-field amplitudes, Opt. Lett. **30**, 2805 (2005).